

# Interactions of the wakes of two spheres placed side by side

L. Schouveiler<sup>a</sup>, A. Brydon<sup>b</sup>, T. Leweke<sup>a,\*</sup>, M.C. Thompson<sup>b</sup>

<sup>a</sup> *Institut de recherche sur les phénomènes hors équilibre (IRPHE), CNRS/Universités Aix-Marseille I & II, 49, rue F. Joliot-Curie, 13884 Marseille cedex 13, France*

<sup>b</sup> *Fluids Laboratory for Aeronautical and Industrial Research (FLAIR), Department of Mechanical Engineering, Monash University, Victoria 3800, Australia*

Received 2 May 2003; accepted 15 May 2003

---

## Abstract

The periodic coupled wakes of two spheres, placed side by side in a uniform stream at low Reynolds numbers, are studied experimentally and by Direct Numerical Simulations. Distinctly different regimes of interaction are observed, depending on the separation distance between the spheres. For touching spheres, a single wake is found. At very small separations, it is shown through numerical simulations that the wakes interact strongly and the combined wake is offset with respect to the centreplane between the spheres. The wake is presumably metastable, probably resulting in the strong structural vibrations of the spheres observed in the present experiments for this regime. At slightly larger separations, the two wakes still interact strongly, and out-of-phase shedding occurs predominantly. In-phase shedding is observed experimentally for intermediate gap sizes, whereas DNS does not reveal a preferred phase difference between the two wakes. At distances above three sphere diameters, shedding is uncorrelated. Variations of the critical Reynolds number and shedding frequencies with separation distance are shown.

© 2003 Elsevier SAS. All rights reserved.

*Keywords:* Sphere wake; Vortex shedding; Coupled wakes

---

## 1. Introduction

The flow around a sphere at low Reynolds numbers, and the transitions between different flow regimes occurring, as the flow velocity is increased, has attracted a renewed interest in recent years [1–5]. Although the sphere is the simplest geometry representing a three-dimensional bluff body, a number of applications exist, ranging from the aerodynamics of sports balls to particle-laden or multi-phase flows, the latter two often involving quite low Reynolds numbers. When particle or bubble densities in these flows increase, the wakes of the immersed bodies start to influence each other.

The wake of a single sphere (diameter  $d$ ) placed in a uniform flow (velocity  $U$ ) undergoes a series of transitions, when increasing the Reynolds number  $Re = Ud/\nu$  ( $\nu$ : kinematic viscosity), which are now well documented. Up to  $Re \approx 210$ , the sphere wake is axisymmetric and exhibits a recirculation region in the form of a vortex ring. Above this value, axisymmetry is lost, and the wake takes the form of two counter-rotating streamwise vortices, which are stationary and present a planar symmetry. Time-dependence first comes in at  $Re \approx 280$ , when the wake starts to oscillate, accompanied by the periodic shedding of vortex loops, which still retain the planar symmetry of the previous stationary regime. This symmetry and the strict periodicity of the wake are in turn lost above  $Re \approx 360$ , when low frequency modulations and variations in the orientation of the plane of symmetry appear.

In this paper, we consider the interaction of the wakes of two stationary spheres, placed side by side in a uniform flow (Fig. 1(a)), for Reynolds numbers between 200 and 350, i.e., in a range where, for the case of a single sphere, the transition

---

\* Corresponding author.

*E-mail address:* [Thomas.Leweke@irphe.univ-mrs.fr](mailto:Thomas.Leweke@irphe.univ-mrs.fr) (T. Leweke).

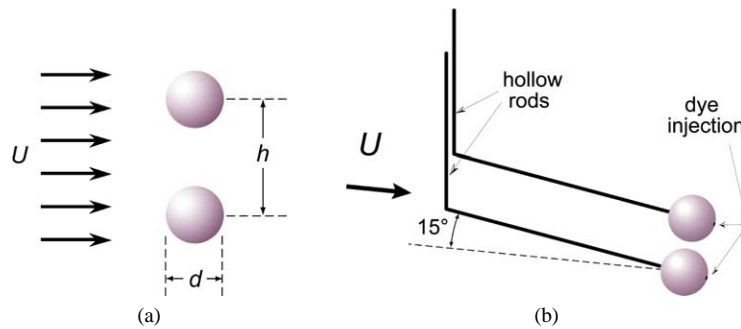


Fig. 1. (a) Flow configuration considered. (b) Schematic of the experimental set-up.

from a stationary to a periodic wake occurs. Previous studies on sphere wake interactions include the numerical simulations by Kim, Elgobashi and Sirignano [6] of the stationary flow past two side-by-side spheres for  $Re$  up to 150, and experimental visualisations and force measurements by Tsuji, Morikawa and Terashima [7] for two or three spheres in various arrangements.

Due to its relevance to many engineering applications, the related problem of interference of circular cylinder wakes has been attracting much more attention, see, e.g., [8–10] or the more recent reviews [11–13]. These studies show that the degree of interaction of two wakes depends mainly on the separation distance between the bodies. For two cylinders in a side-by-side arrangement, the following interference regimes of vortex shedding are reported for increasing separation distance: single wake (for touching cylinders), two asymmetric wake states with intermittent changeover between them, and locked modes where the vortex shedding behind both cylinders can be in phase or (predominantly) out of phase.

## 2. Technical details

The flow was studied both experimentally and by Direct Numerical Simulation (DNS). Experimental visualisations were obtained in a water channel of cross section  $12 \times 15 \text{ cm}^2$ . The two Teflon spheres of diameter  $d = 10 \text{ mm}$  were held from upstream by two rigid bent hollow rods (external diameter 1.5 mm), connected to an adjustable support outside the test section, which allowed variation of the distance  $h$  between the centres of the spheres. The part of each rod attached to the respective sphere was inclined by about  $15^\circ$  with respect to the direction of the free stream, in a plane perpendicular to the line joining the two sphere centres (see Fig. 1(b)). Fluorescent dyes were injected through small downstream holes connected through a channel across the spheres with the hollow upstream support rods. The flow was illuminated by the light of a 5 W Argon ion laser and recorded on standard VHS video. Quantitative measurements of wake frequencies were obtained using the same system of spheres and supports in a low-speed low-turbulence wind tunnel with a  $25 \times 25 \text{ cm}^2$  cross section. The free stream velocity  $U$  was measured by Laser Doppler Anemometry (LDA) in the section containing the sphere centres, thus accounting automatically for blockage and boundary layer growth. Wake spectra were obtained from LDA measurements made approximately  $5d$  downstream of the spheres. The two parameters governing the flow are the Reynolds number based on the diameter of one sphere and the non-dimensional separation distance  $h/d$ . The latter parameter was varied between 1 (touching spheres) and 4.6.

Direct Numerical Simulations of the two-sphere wake were performed for  $Re = 300$  and different separation distances using a three-dimensional spectral-element code. Use of a high-order splitting method results in second-order temporal accuracy. The rectangular simulation domain extends from  $4d$  upstream to  $20d$  downstream, and has cross-section dimensions of  $8d + h$  and  $8d$  in the directions parallel and perpendicular to the line joining the two spheres, respectively. The computational mesh contains up to 1764 seventh-order spectral elements with up to 626 000 nodes, whose density is maximum in the vicinity of the sphere and in the near wake where velocity gradients are highest. Full details of the method, including extensive code validation, can be found in [14].

## 3. Results

### 3.1. Periodic wake of a single sphere – clarification

From the earliest studies of sphere wakes [15] until recently, knowledge about the structure of the wake of a single stationary sphere at low Reynolds number was principally based on results from flow visualisations like the example shown in Fig. 2(a).

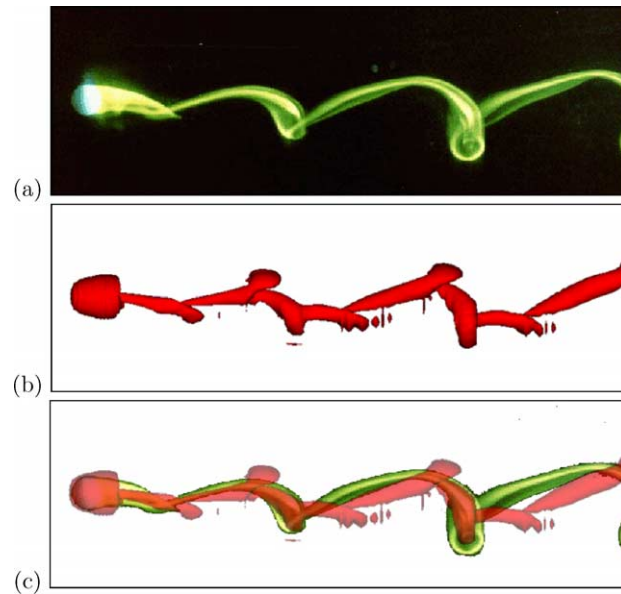


Fig. 2. Side views of the periodic wake of a single sphere at  $Re = 300$ . (a) Dye visualisation; (b) vortical structures from DNS visualised using the method proposed in [16]; (c) superposition of the two.

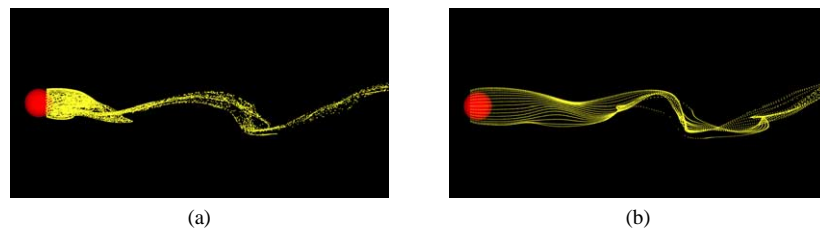


Fig. 3. Sphere wake from DNS at  $Re = 300$  visualised by particle streaklines. Particles are continually introduced (a) at  $120^\circ$  from the front stagnation point and  $0.1d$  from the sphere surface, and (b) at  $60^\circ$  and  $0.2d$ .

The majority of visualisations in the literature seem to indicate that, in the approximate range  $280 < Re < 360$ , the sphere wake is characterised by the periodic shedding of vortex loops of planar symmetry. The regions between successive loops show pairs of smoothly curved threads of dye whose ends are attached to the vortex loop heads. Johnson and Patel [1], who studied the sphere wake using Direct Numerical Simulation, were the first to show that these regions between the loops actually also contain vortical structures in the form of what they call induced hairpin vortices. These structures are also found in the present numerical study, as shown in Fig. 2(b). Although one must always be careful when interpreting visualisation pattern in terms of vortical structures, especially in three-dimensional flows with high Schmidt number, the observed discrepancy between the visualisation pattern and the calculated vortical structures in the sphere wake is quite surprising (Fig. 2(c)). Knowing that all vorticity is generated at the surface of the sphere, where the dye is also injected, one may wonder why there is no trace of the ‘induced’ hairpin vortices in the dye visualisations.

The answer may be linked to the particular way the sphere wake is visualised. In most studies, dye is either painted on the sphere before an experiment, it is injected near the downstream stagnation point, or the sphere is moved through a cloud of dye. In all these cases, the dye visualising the asymptotic wake structure is mainly the one that was trapped for some time in the (oscillating) recirculation region behind the sphere, whereas the dye in the boundary layer on the front part of the sphere up to separation is very quickly washed away. As a consequence, very often an important fraction of the vorticity generated at the surface of the sphere is not dyed, and it is believed that this undyed vorticity is responsible for the formation of the ‘induced’ hairpin vortices.

As an illustration, Fig. 3 shows numerically calculated streaklines, obtained by continually introducing massless particles into the flow and following their positions in time. In Fig. 3(a), particles are introduced into the recirculation region, and the resulting pattern is very close to the experimental dye visualisation in Fig. 2(a), i.e., there is almost no indication of structures between the primary loop heads. When particles are introduced upstream of the boundary layer separation (Fig. 3(b)), the

streaklines now exhibit a pronounced kink in the region between loops, i.e., where numerical simulations suggest the existence of additional vortical structures. Further simulations have shown a great sensitivity of the streakline pattern with respect to the location of injection of the particles. An experimental visualisation in which dye is continually fed into the flow from the entire surface of the sphere, would probably resemble much closer the numerical visualisation of Fig. 2(b).

Although the possible discrepancy between dye pattern and vorticity is well known, it is particularly striking for the sphere wake. We believe it is worth pointing out that the ‘classical’ picture of the periodic sphere wake as a series of smooth vortex loops, based on results of a certain type of flow visualisation, is a very poor representation of the real wake of a sphere.

### 3.2. Wake regimes of the two-sphere system

For Reynolds numbers in the range corresponding to a periodic single-sphere wake, experimental flow visualisations (Fig. 4) and vorticity plots from Direct Numerical Simulation (Figs. 5–8(a)) have shown the existence of different regimes of wake interaction for two spheres placed side by side. The observed coupling mode depends on the sphere spacing. The various regimes are presented in the following as a function of the non-dimensional distance  $h/d$ .

#### 3.2.1. Touching spheres ( $h/d = 1$ )

When the two spheres are touching, they act as a single bluff body. In its wake, large-scale vortex loops are shed on both sides of the plane containing both sphere centres, as shown in the experimental and numerical visualisations in Figs. 4(a), (b) and 6, respectively. In the experiments, the loops on both sides were generally shed with a phase difference not far from  $90^\circ$ , which, in the side view in Fig. 4(b), results in a pattern similar to images of a two-dimensional Kármán vortex street behind a circular cylinder. This is in agreement with earlier observations [7] of the wake behind three touching spheres. In the numerical simulations, however, the loops on both sides of the wake are shed simultaneously, as seen in Fig. 6 (bottom). The vortex loops have an approximately planar symmetry with respect to the plane separating the two spheres. Nevertheless, the plan view of the wake obtained from DNS (Fig. 6 top) reveals that the loops twist right and left alternatively as they are shed into the wake. This means that the actual period of the wake is twice the period of loop shedding. This is also clearly visible in the vorticity pattern in the symmetry plane shown in Fig. 5(a), where the streamwise wavelength of the wake is found to be twice the distance between the almost circular patches of vorticity marking the location of the loops. Nevertheless, most of the fluctuation energy of the wake has the frequency of the loops, which is also the principal frequency detected in the experiments. As shown below, its value is significantly higher for this “merged” two-sphere wake than for the other regimes with non-zero gaps between the spheres, and which are all characterized by the existence of two identifiable wakes, one behind each sphere. It is difficult to detect in the dye visualisations (Fig. 4(a) and (b)) if the alternate twisting of loops also happens in the experiments.

The differences between experiment and DNS for the touching spheres may partly be caused by the method of fixing the spheres in the former. It is also possible that the wake in the simulations has not reached its asymptotic state. However, the symmetrical wake pattern in Fig. 6 was maintained during the last 20 periods of the simulation and appeared to be relaxing

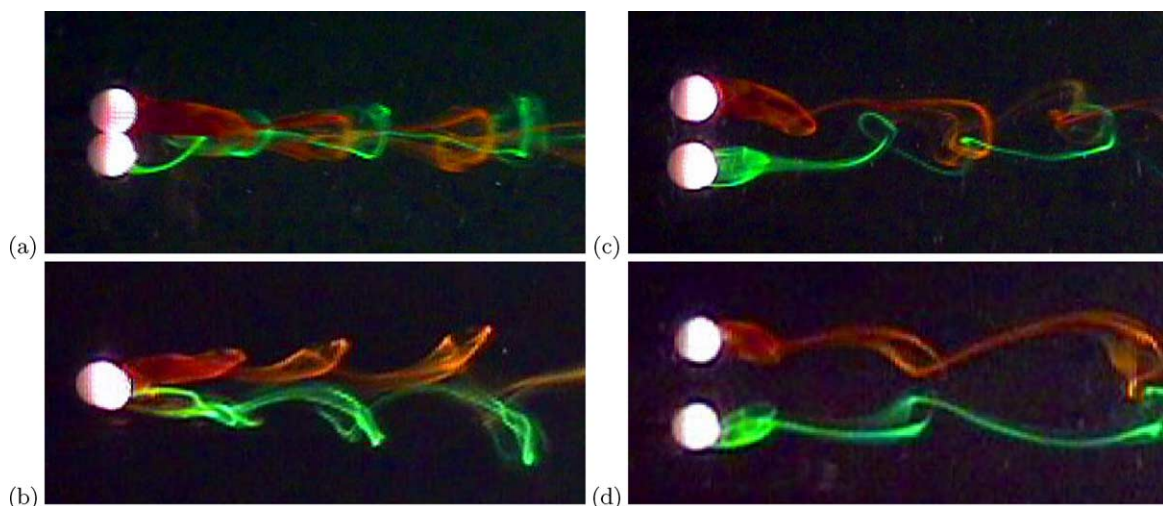


Fig. 4. Dye visualisation of the coupled wakes of two spheres at  $Re = 330$ . (a) and (b)  $h/d = 1.0$ , top and side view, respectively; (c)  $h/d = 1.6$ ; (d)  $h/d = 1.9$ .

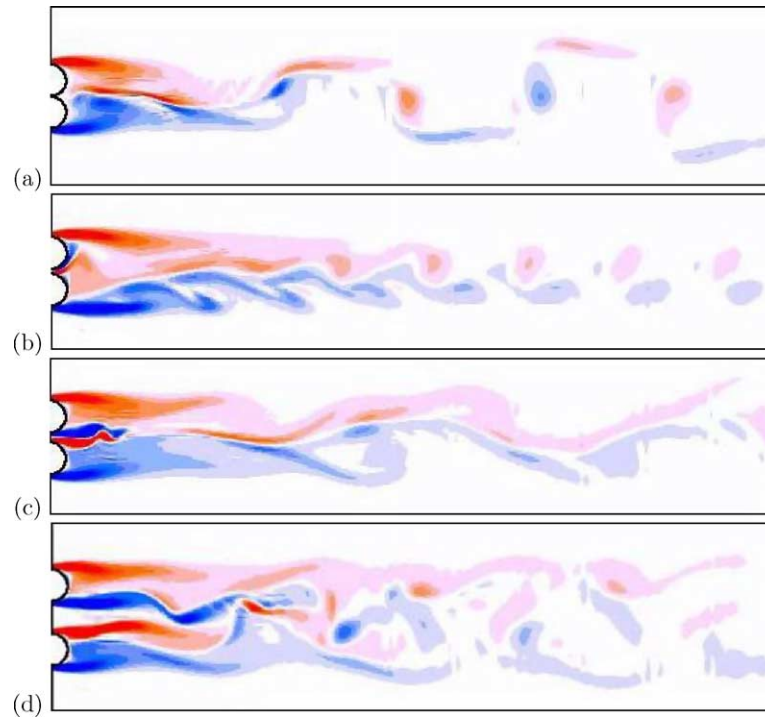


Fig. 5. Greyscale vorticity contours in the plane aligned with the flow direction passing through the two spheres, obtained from DNS at  $Re = 300$ . (a)  $h/d = 1.00$ , (b)  $h/d = 1.15$ , (c)  $h/d = 1.30$ , (d)  $h/d = 2.00$ .

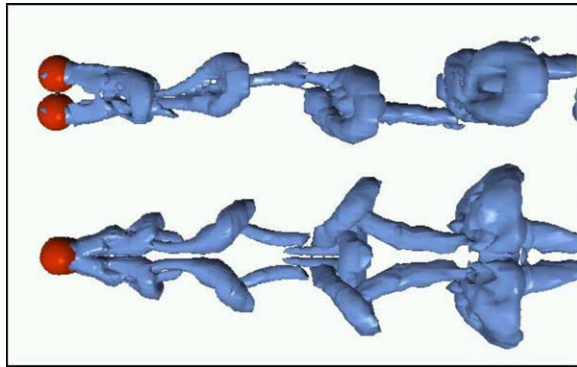


Fig. 6. Simultaneous top and side view visualisations of vortical structures in the wake of two touching spheres ( $h/d = 1.00$ ), from DNS at  $Re = 300$ , using the method of Jeong and Hussain [16].

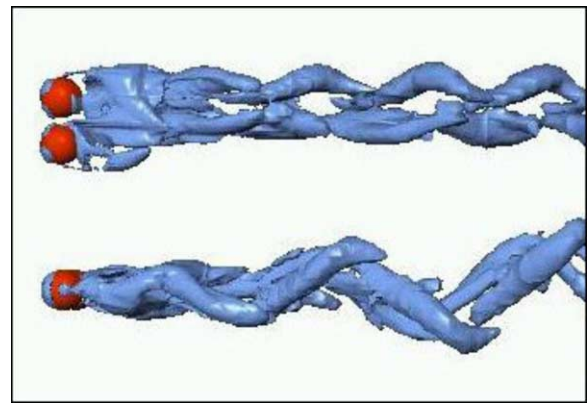


Fig. 7. Same as Fig. 6 for  $h/d = 1.15$ .

towards a purely periodic state. Finally, the difference in Reynolds numbers (which was 330 for the flow visualisations and 300 in the simulations) may also have a non-negligible effect.

### 3.2.2. Small gaps ( $1.0 < h/d < 1.3$ )

In the experimental study, it was not possible to obtain reliable results concerning the coupled sphere wakes for very small but non-vanishing gaps. This was due to the presence of strong vortex-induced mechanical vibrations of the sphere-support systems at these low separations in the particular experimental arrangement used (see Fig. 1(b)). However, it was possible to perform numerical simulations for gap ratios within this region. Fig. 5 shows greyscale contours of the vorticity component normal to the centreplane passing through the two spheres. For the gap ratios  $h/d = 1, 1.3$  and  $2.0$ , the wake is symmetrical about the centreline, except for the  $180^\circ$  phase shift in period between the two sides of the wake.

The wake structure for  $h/d = 1.15$  does not have this symmetry. This wake developed from a stationary flow over many periods. At a time during the evolution it switched rather suddenly to the state shown in this figure. The fluid passing through the gap hugs the surface of the top sphere and only separates after it reaches the rear of the sphere. This is likely to be related to the Coanda effect for which a jet of fluid remains attached to the surface of a curved body as the surface curves away from the flow direction. For the numerical simulations, this wake configuration appears to be stable. However, the symmetrical situation with the jet attached to the other sphere must be equally stable, and hence wake must be bistable in this regime. Presumably in the experiments, the existence of this bistable state can lead to a strong fluid-structure interaction with the wake switching between these two distinct metastable states causing strong structural vibration. Of note is that the shedding frequency in the far wake is much higher than that for neighbouring gap ratios.

Fig. 7 show isosurfaces highlighting the wake structure using the visualisation method proposed in [16]. This effectively depicts the vorticity structure of the wake, consistent with the cross-sectional vorticity contours shown in Fig. 5(b). The loss of symmetry about the midplane between the spheres is clearly evident, with the wake displaced to one side.

Similarly, two bistable asymmetric states have been observed in coupled circular cylinder wakes. Intermittent changeovers between them have been reported [17], occurring on a time scale several orders of magnitude longer than the vortex shedding period. Thus, observation of such regime exchange would require a much longer simulation time.

### 3.2.3. Intermediate gaps ( $1.3 < h/d < 3$ )

In this range of separation distances (and for higher values), each sphere has a recognizable individual wake, and the overall flow is found to be symmetric with respect to the central plane between the spheres. For intermediate gaps, the two wakes are more or less strongly coupled. In the case of a single sphere, the orientation of the plane of symmetry of the periodic wake is arbitrary; it is determined by the initial conditions of the flow or (in experiments) by the presence of a symmetry-breaking support system. In the present experiments, the plane of symmetry for an isolated sphere wake was found to be aligned with the plane containing the support rod. In the two-sphere case, the second sphere introduces a preferred direction for the orientation of the wake. Results from DNS, i.e., for configurations without support rod, indicate that in this regime of strong coupling the symmetry plane of each wake tends to align with the plane containing the sphere centres. This implies an overall planar symmetry of the combined wake, and the downstream ends of the vortex loops shed from each sphere are found to curve towards the wake centreline, as illustrated in the visualisations in Figs. 4(c), (d). In agreement with this, the lift force on each sphere is found to be oriented in a direction aligned with the plane of symmetry in the asymptotic wake, as shown by the numerical results in Fig. 8(c). In the present experiments, there was a competition between the influence of the support rods and the proximity of the second sphere, tending to align the wakes vertically or horizontally, respectively. As the gap ratio varies from 1.3 to about 3, the individual wake symmetry planes turn from the horizontal to the vertical direction through a series of intermediate V-shaped configurations.

The present results indicate that the regime of coupled wakes can be further subdivided into two parts. The visualisation in Fig. 4(c) represents the coupled wake pattern for separation distances  $h/d$  in the approximate range 1.3–1.7. Here, shedding from the two spheres occurs with a phase shift of  $180^\circ$ . The proximity of the two spheres in this regime leads to a mutual deformation of their respective wakes. Fig. 4(c) shows that the dye filaments connecting two successive heads of the vortex loops shed from one sphere are distorted by the flow induced by the loop from the other sphere's wake. It was shown above that the region of the threads contain additional vorticity structures not visualised by the dye, and the interaction between these 'induced' vortices of one sphere wake with the primary loop from the other appears to be responsible for the strong deformations. This leads to structures that have a streamwise wavelength of half the one initially found in each separate wake. The experimental observation of out-of-phase shedding is well confirmed by the numerical results in Fig. 8. Fig. 8(a) shows the strong interaction between vortex structures from each individual wake, and the  $180^\circ$  phase shift is clearly visible in the temporal evolution of the drag coefficients for both spheres.

For slightly higher gap ratios, i.e., for  $1.7 < h/d < 3$  approximately, the interaction between the two wakes is much weaker. The wake of each sphere is found to exhibit a downstream evolution very similar to the one for an isolated single sphere, as illustrated in the visualisation in Fig. 4(d). However, a coupling still exists: both wakes are again symmetric with respect to the plane containing the sphere centres, but now the periodic shedding of vortex loops occurs simultaneously, leading to an additional planar symmetry of the overall wake with respect to the plane between the spheres. In the experiments, this in-phase shedding was systematically observed in this range of  $h/d$ . In the numerical simulations, other phase angles between the two wakes were also observed for  $h/d = 2$  ( $\sim 180^\circ$  phase shift) and  $h/d = 2.5$  ( $\sim 90^\circ$  phase shift), where the flow was started from rest and from an initial condition built from two single-sphere wakes, respectively. At present, it is not clear if different metastable states exist for the coupled sphere wakes in this parameter range, or if the presence of the support structures somehow selects the in-phase shedding in the experiments, whereas in the idealised flow the phase difference might be more or less random. This point is under investigation.

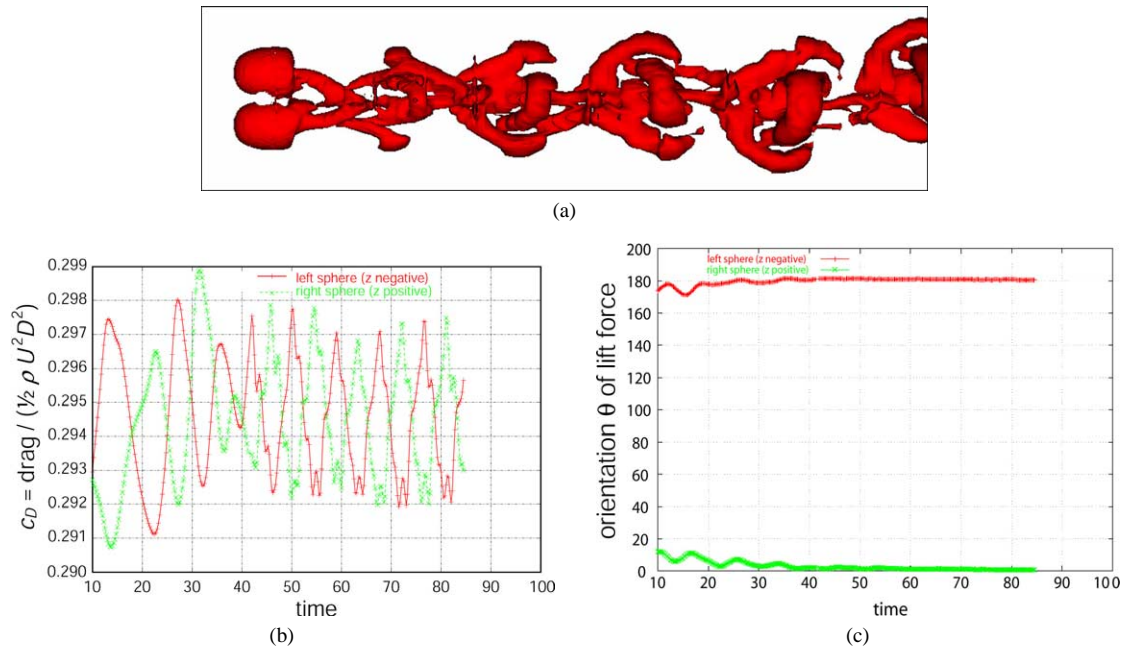


Fig. 8. (a) Wake structure at  $Re = 300$  and  $h/d = 1.5$ , from DNS. (b) Time dependent drag coefficients and (b) directions of the lift force for the two spheres.  $\theta = 0$  and  $\theta = 180^\circ$  are parallel to the line joining the spheres, the time unit is  $d/U$ .

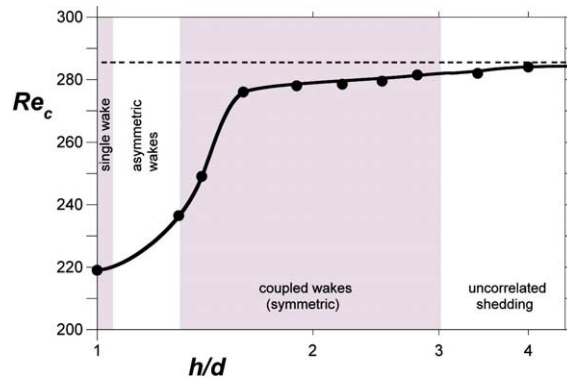


Fig. 9. Critical Reynolds number for the onset of time-dependent (periodic) wake structure, as a function of separation distance (from experiment). The dotted line represents the value measured for a single sphere. Note the logarithmic abscissa.

### 3.2.4. Large gaps ( $h/d > 3$ )

For separation distances larger than about three sphere diameters, both experiment and DNS show no preferred phase difference of the shedding from the two spheres. This result is in agreement with the drag measurements of Chen and Lu [18]. In the experiments, the orientation of the plane of symmetry of each sphere wake is now determined by the geometry of the support structure, i.e., aligned with the (vertical) plane of the bent support rod, as for the single sphere case. In the DNS, these orientations are basically random in this range of separation distances. A very weak coupling is nevertheless still observed at  $h/d = 3.5$ , leading to a slow drift of the orientation of the plane of symmetry for each separate wake towards the line going through both sphere centres, similar to the situation observed for the previous regimes with stronger coupling.

### 3.3. Quantitative results

Figs. 9 and 10 show results from experimental LDA measurements and DNS calculations characterizing the different regimes of sphere wake interaction.

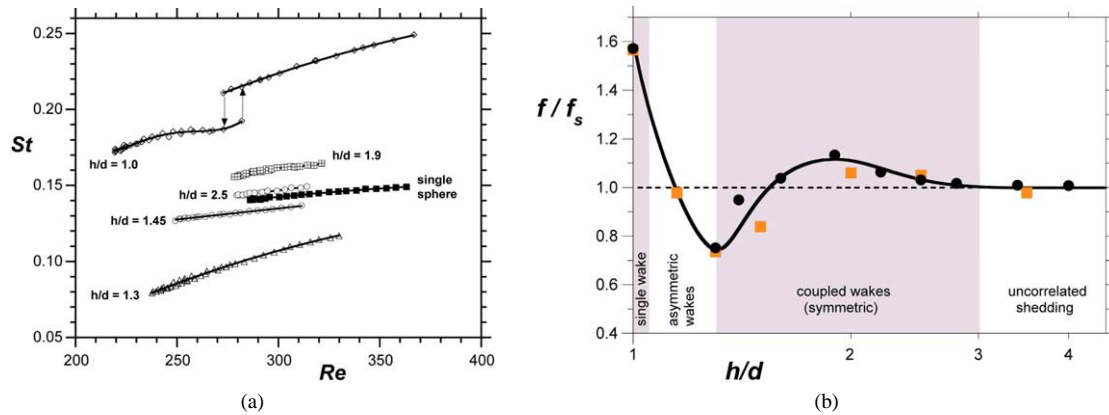


Fig. 10. Frequencies of the coupled sphere wakes; (a) Strouhal numbers as a function of Reynolds number for different separation distances (experiment); (b) frequency ratio as a function of separation distance at  $Re = 300$  (●: experiment, ■: DNS,  $f_s$ : frequency of single-sphere wake).

The critical Reynolds number for the onset of time-dependent periodic wake flow is shown in Fig. 9 as function of the separation distance. For touching spheres, it is found to be  $Re_c = 219$ . This case may be compared to the flow around a short cylinder with free hemispherical ends and aspect ratio 2, investigated in [19]. There, a significantly lower value of  $Re_c = 155$  is found. As soon as the spheres are moved apart, the critical  $Re$  increases rapidly within the regime of strong coupling and out-of-phase shedding, to reach a value close to 280. From thereon, the variation slows down, it gradually approaches the value of  $Re_c = 283$  measured for a single sphere with the present experimental set-up.

The shedding frequencies of the coupled wakes are plotted in Fig. 10 in the form of Strouhal numbers  $St = fd/U$  ( $f$ : wake frequency). Fig. 10(a) shows the experimentally observed frequency variations in the periodic regimes for various values of  $h/d$ . The different onset Reynolds numbers are clearly seen, as well as an interesting hysteresis phenomenon occurring for the case of touching spheres around  $Re = 280$ . The extent of the periodic regime varied significantly in the present experiments. Based on known results for circular cylinder wakes, it is likely that the upper limit of the periodic regime is very sensitive to small imperfections of the experimental set-up. The observed variations therefore have to be interpreted with some reservations.

For a fixed Reynolds number, the Strouhal number is found to vary smoothly with gap ratio for symmetric coupled wakes ( $h/d > 1.3$  in Fig. 10(b)). It increases in the regime of strong coupling, reaching a maximum just under  $h/d = 2$ , from where it then decreases again, asymptoting the value for a single sphere at large separations. The DNS values show the same overall trend, and are very close to the experimental results. The Strouhal number obtained numerically for a single sphere is  $St_s = 0.136$ , in excellent agreement with other recent studies [1,2].

When the gap ratio decreases below 1.3 into the regime of asymmetric coupled wakes, a sharp increase in the Strouhal number is observed. When the spheres finally touch, the wake frequency is much higher ( $St = 0.224$ ) than for the other regimes, and closer to the one for a circular cylinder of diameter  $d$ . It is interesting to note that, for a cylinder of aspect ratio 2 with free hemispherical ends, the regime of periodic single-frequency shedding only extends from  $Re \approx 155$  to  $Re \approx 190$  [19], whereas the wake of the two touching spheres (a priori a rather similar geometry) is periodic in the range  $219 < Re < 370$  (Fig. 10(a)).

#### 4. Conclusions

Experiments and Direct Numerical Simulations of the wakes of two stationary spheres placed side by side in a uniform flow at low Reynolds numbers, have revealed the existence of different regimes of interaction, as a function of the spheres' separation distance. When increasing this distance from one diameter (touching spheres), one successively observes a single wake, two coupled wakes with out-of-phase shedding, two wakes with in-phase shedding (mainly in the experiments), and independent shedding from both spheres. This sequence of regimes is similar to the well documented case of two interacting cylinder wakes.

The critical Reynolds number for the onset of shedding decreases rapidly with decreasing separation distance, once the latter drops below two sphere diameters. At a given Reynolds number, the wake frequency varies smoothly with separation distance in the range where two separate wakes can be identified. As the spheres are brought closer together, it first increases above, then decreases below the value for an isolated sphere. For touching spheres, the frequency of oscillation is closer to that for a circular cylinder, and a hysteresis in the Strouhal–Reynolds number relationship is found around  $Re = 280$ . Good agreement exists between experimental and numerical results.

As mentioned in the introduction, this study of fixed sphere wake interaction may have relevance for the characterisation of two-phase (bubbly or particle-laden) flows. As a further step in this direction, interactions of freely moving spheres, with the additional effects of sphere inertia, will be considered next. Investigations of freely falling and rising spheres are currently underway.

### Acknowledgement

This work was supported by collaborative research grants from the French Centre National de la Recherche Scientifique (CNRS, grant no. DRI 11721) and from the Australian Research Council (ARC, grant no. LX0242362).

### References

- [1] T.A. Johnson, V.C. Patel, Flow past a sphere up to a Reynolds number of 300, *J. Fluid Mech.* 378 (1999) 19–70.
- [2] A.G. Tomboulides, S.A. Orszag, Numerical investigation of transitional and weak turbulent flow past a sphere, *J. Fluid Mech.* 416 (2000) 45–73.
- [3] B. Ghidersa, J. Dušek, Breaking of axisymmetry and onset of unsteadiness in the wake of a sphere, *J. Fluid Mech.* 423 (2000) 33–69.
- [4] M.C. Thompson, T. Leweke, M. Provansal, Kinematics and dynamics of sphere wake transition, *J. Fluids Structures* 15 (2001) 575–585.
- [5] L. Schouveiler, M. Provansal, Self-sustained oscillations in the wake of a sphere, *Phys. Fluids* 14 (2002) 3846–3854.
- [6] I. Kim, S. Elgobashi, W.A. Sirignano, Three-dimensional flow over two spheres placed side by side, *J. Fluid Mech.* 246 (1993) 465–488.
- [7] Y. Tsuji, Y. Morikawa, K. Terashima, Fluid-dynamic interaction between two spheres, *Int. J. Multiphase Flow* 8 (1982) 71–82.
- [8] P.W. Bearman, A.J. Wadcock, The interaction between a pair of circular cylinders normal to a stream, *J. Fluid Mech.* 61 (1973) 499–511.
- [9] C.H.K. Williamson, Evolution of a single wake behind a pair of bluff bodies, *J. Fluid Mech.* 159 (1985) 1–18.
- [10] I. Peschard, P. Le Gal, Coupled wakes of cylinders, *Phys. Rev. Lett.* 77 (1996) 3122–3125.
- [11] W. Jester, Y. Kallinderis, Numerical study of incompressible flow about fixed cylinder pairs, *J. Fluid Structures* 17 (2003) 561–577.
- [12] J.F. Ravoux, A. Nadim, H. Haj-Hariri, An embedding method for bluff body flows: interactions of two side-by-side cylinder wakes, *Theor. Comp. Fluid Dyn.* 16 (2003), in press.
- [13] S.J. Xu, Y. Zhou, R.M.C. So, Reynolds number effects on the flow structure behind two side-by-side cylinders, *Phys. Fluids* 15 (2003) 1214–1219.
- [14] A. Brydon, High-order simulation of swirling and compact bluff-body flows, Ph.D. thesis, Department of Mathematics and Statistics, Monash University, Melbourne, Australia, 2000.
- [15] W. Möller, Experimentelle Untersuchungen zur Hydrodynamik der Kugel, *Phys. Z.* 39 (2) (1939) 57–80.
- [16] J. Jeong, F. Hussain, On the identification of a vortex, *J. Fluid Mech.* 285 (1995) 69–94.
- [17] H.J. Kim, P.A. Durbin, Investigation of the flow between a pair of circular cylinders in the flopping regime, *J. Fluid Mech.* 196 (1988) 431–448.
- [18] R.C. Chen, Y.N. Lu, The flow characteristics of an interactive particle at low Reynolds numbers, *Int. J. Multiphase Flow* 25 (1999) 1645–1655.
- [19] L. Schouveiler, M. Provansal, Periodic wakes of low aspect ratio cylinders with free hemispherical ends, *J. Fluids Structures* 15 (2001) 565–573.